ACS SyntheticBiology

pubs.acs.org/synthbio Letter

Smart Microbial Cells Couple Catalysis and Sensing to Provide High-Throughput Selection of an Organophosphate Hydrolase

Ramesh K. Jha* and Charlie E. M. Strauss*

Cite This: *ACS Synth. Biol.* 2020, 9, 1234–1239 Read Online

ACCESS | Metrics & More | Article Recommendations | Supporting Information

ABSTRACT: Enzyme engineering for gain of function requires navigating a large combinatorial sequence space efficiently. Typically, many mutations are needed to get significant improvements, while a single "bad" mutation can inactivate the enzyme. To establish high-throughput screening and achieve enhanced resolution between two variants, genetic libraries of the organophosphate hydrolase enzyme paraoxonase 1 (PON1) were rapidly screened *via* an engineered positive-feedback circuit: a *p*-nitrophenol (PNP)-specific transcription factor (TF) regulated expression of PON1, which catalyzed paraoxon breakdown and PNP production. Rare active mutant colonies, picked by simple visual fluorescence of a PON1−green fluorescent protein (GFP) fusion, were characterized. In a single screening round, high (library-scale) throughput enabled the discovery of enhanced paraoxon degradation activity in PON1, including structurally unexpected mutations.

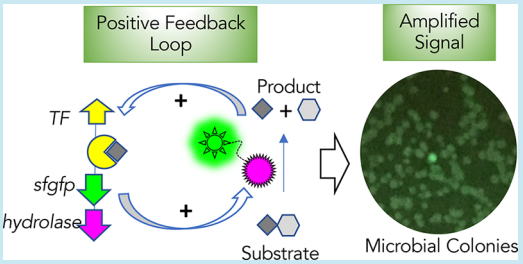

KEYWORDS: *whole-cell biosensor, PNP sensor, paraoxon, PON1, high-throughput screening, positive-feedback circuit*

Diverse industrial applications demand enhanced enzymes that can hydrolyze non-natural substrates (*e.g.*, therapeutics,[1] renewable energy,[2] biomanufacturing,[3] and environment cleanup[4]). Critically, enzyme discovery and engineering need high-throughput methods to rapidly screen very large numbers of sequences for any novel function or substantial gain in function.[5] Since *p*-nitrophenol (PNP) is a chromogenic chemical leaving group, it has become a ubiquitous reporter for hydrolytic catalyst characterization. However, a spectrophotometric monitoring format is limited to low throughput, typically a 96- to 384-well plate with one well for each enzyme variant.[6] Instead, we previously reported a "smart" microbial cell (SMC) technology and single-cell monitoring of PNP using a computationally redesigned PobR transcription factor (TF) regulating expression of a fluorescent reporter.[7] We showed that the sensor−reporter system could detect organophosphate (OP) hydrolysis, and the single-cell fluorescence was correlated with the published *in vitro* enzymatic activity.[7]

In the present work, we extended this technology to library-based screening of a mammalian serum paraoxonase 1 (PON1) enzyme.[8] The previous state of the art in PON1 performance was achieved mainly by judicious mergers of point mutations chosen in the vicinity of the catalytic pocket.[9] The individual mutations L69V, H115W, and V346A enhanced the catalytic efficiency of PON1 for hydrolysis of OPs by 4- to 16-fold.[10] Its variants have been adapted for catalysis and stereoselectivity against multiple OPs.[11] Directed evolution of PON1 *via* DNA shuffling[9] or error-prone PCR[12] have discovered mutations that improve the expression, substrate specificity, and catalytic efficiency. However, without a means for direct selection for enhanced activity, the library size and throughput are bottlenecked by the need for activity assays with individual genotypes expressed and lysed in individual sample wells.[13] Our SMC technology allows for catalysis and sensing in a microbe.[7,14] For a practical library application, we simplified and improved the signal-to-noise ratio of the biosensor. This was achieved by gene fusion of *pon1* and *gfp* reporter so that the TF also regulated the enzyme expression (Figures 1A and S1). This fusion is expected to have three distinct effects. First, it provides positive feedback, such that with greater activity, more PON1 is expressed, which in turn further "feeds" the activity. The feedback would therefore enhance the sensitivity to weak activity by raising the signal above both the ambient background and leaky expression of the GFP reporter. Notably, when the PON1 is inactive there is no positive feedback, so basal expression is not increased by the feedback. Second, the feedback amplifies the already-present correlation between activity and GFP expression.[15] Third, for suitably chosen GFP, the fluorescence signal conveniently reports the amount of fused PON1 present, allowing normalization for specific activity.

A weakly folding GFP placed at the C-terminus *after* a protein of interest is known to function as folding reporter, since a misfolded (insoluble) N-terminal protein will interrupt the formation of the subsequently translated GFP chromo-

Received: January 14, 2020
Published: May 5, 2020

https://dx.doi.org/10.1021/acssynbio.0c00025
ACS Synth. Biol. 2020, 9, 1234−1239

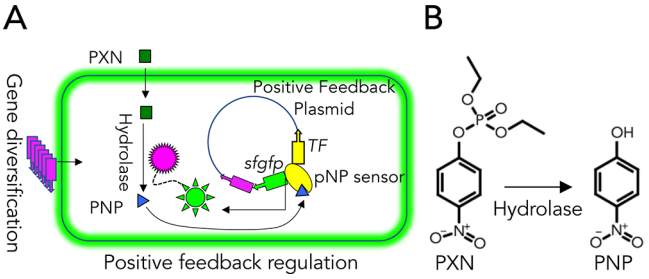

Figure 1. "Smart" microbial cell (SMC) technology for paraoxon (PXN) hydrolysis. (A) Cartoon illustrating the technology. The flow scheme shows entry of PXN into a bacterial cell, enzymatic hydrolysis for *p*-nitrophenol (PNP) release, activation of the PNP sensor, and accumulation of superfolder green fluorescent protein (sfGFP) in the cell resulting in a gain in cell fluorescence. Since *sfgfp* (green arrow) and the gene for the PXN hydrolase (magenta arrow) are in the same open reading frame, a positive feedback loop is created wherein the enzyme regulates its own expression. Diversified genes can be cloned in the positive-feedback plasmid. (B) PXN hydrolysis and the PNP leaving group.

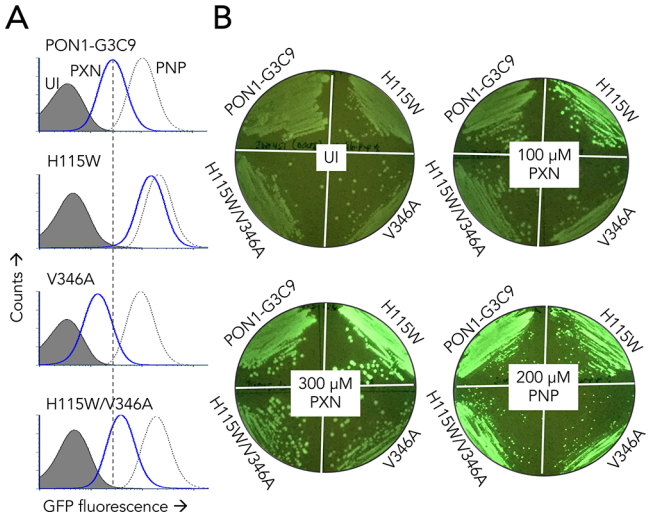

Figure 2. Establishing SMC technology in *E. coli*. (A) Histograms from flow cytometry showing the *E. coli* JW0451 strain (Δ*acrB*) transformed with the positive-feedback plasmid expressing a PON1 variant and grown under different induction conditions. Uninduced (UI) (gray): background fluorescence from cells without any PNP source. PXN (blue, solid line): exogenous PXN (1.6 mM) conversion by enzyme and product PNP activating the TF. The dashed line across the histograms serves as an eye guidance for comparison of the PXN histograms across different variants. PNP (dotted line): TF induced by exogenously supplemented PNP (200 μM) as a control/reference. The *x* axes are on a logarithmic scale. Figures were created using FCS Express 6 software. (B) Streaked LB agar plates (supplemented with PXN or PNP) with *E. coli* JW0451 strain expressing PON1 variants.

phore.[12,16] In contrast, our assay specifically suppressed that effect using (1) an N-terminal GFP and (2) a superfolder variant of GFP (sfGFP).[17] Thus, it directly reports enzyme activity and not misfolding. However, because of the positive feedback, we still get the benefit of sensing of misfolding since enzyme inactivity means no feedback for enhanced GFP expression.

The sfGFP−PON1 fusion can catalyze the hydrolysis of paraoxon (PXN), where PNP is a leaving group (Figure 1B). On the basis of the catalytic efficiency and cytoplasmic concentration of the hydrolase, PXN hydrolysis results in correlated PNP production inside the microbial cell that ultimately determines activation of the PNP sensor and accumulation of sfGFP in the cells. Our earlier attempts to sense weak activities using an *Escherichia coli*-based SMC showed better resolution with a variant where the efflux pump gene component *acrB* was deleted (strain JW0451[18]). Comparison of SMCs with PON1-G3C9 (nativelike) and the PON1-H115W mutant grown in PXN showed a higher cell fluorescence in the latter (Figure 2A), which is consistent with the higher catalytic efficiency observed for PON1-H115W.[10] The variant PON1-V346A showed lower cell fluorescence than G3C9, even though the mutation was shown to be beneficial for PXN hydrolysis.[10] This could have been due to reduced protein expression and/or stability caused by the mutation. The PON1 version combining the two mutations (H115W/V346A) showed partial recovery of the cell fluorescence in the presence of PXN substrate (Figure 2A and Table S1). Interestingly, when PNP was used as an inducer, such that the expression of sfGFP−PON1 expression was independent of the catalytic efficiency of PON1, modest differences in cell fluorescence were still captured across the PON1 variants, indicating that the V346A mutation could be detrimental to PON1 expression and stability (Figure 2A and Table S1).

When plated on LB agar medium with either PXN or PNP, the SMCs recaptured the fluorescence signal observed in the liquid culture (Figure 2B). At 100 μM PXN, fluorescent colonies were observed only in the case of PON1-H115W, and they showed a gain in fluorescence at 300 μM PXN. SMCs expressing PON1-V346A showed weaker fluorescence than cells expressing PON1-H115W or PON1-G3C9. At 200 μM PNP, irrespective of the PON1 variant, the SMCs were saturated with fluorescence (Figure 2B).

The next step was to move this technology to a library screening. Two separate libraries were created using PON1-H115W as a scaffold. The first library (Lib1) targeted peripheral mutations on loop 69−74 (based on the structural information on PON1 bound to the competitive inhibitor 2-hydroxyquinoline (2HQ); PDB code 3SRG)[19] (Figures 3A,B and Table S2). This loop was expected to play a critical role in the interactions with the substrate/transition state since the loop was disordered in the apo state and gained structure only in the presence of inhibitor in the pocket. The second library (Lib2) consisted of mutations around the catalytic pocket, mostly based on the literature (Figure 3C and Table S3). The goal of Lib2 was to discover any combinatorial solution of synergistic mutations, which earlier were tried mostly as single-point mutations. The theoretical diversity of each library, ∼20 000, was reasonably matched to the SMC-based plate assay, where on a single large Petri dish (135 mm diameter) one can have $\sim 10^4$ isolated colonies demanding two to four Petri dishes for a modest overcoverage.

In order to efficiently screen the PON1 library, the positive-feedback biosensor/biocatalyst plasmid was directly transferred to high-transformation-efficiency DH5α cells (Thermo Fisher). Because of an intact efflux pump, DH5α cells also showed reduction in the basal signal from the scaffold, hence making visual picking in the background of H115W convenient. The SMC libraries harboring two sets of genetic variations showed very different displays on the Petri dish with PXN substrate (330 μM). While Lib1 with the peripheral mutations showed multiple colonies that were distinctly brighter than the surrounding ones (Figure 3D), Lib2 consisting of mutations in the catalytic pocket proved to consist of sequences that were mostly detrimental to the activity. However, a single colony stood out from the rest in a

https://dx.doi.org/10.1021/acssynbio.0c00025
ACS Synth. Biol. 2020, 9, 1234−1239

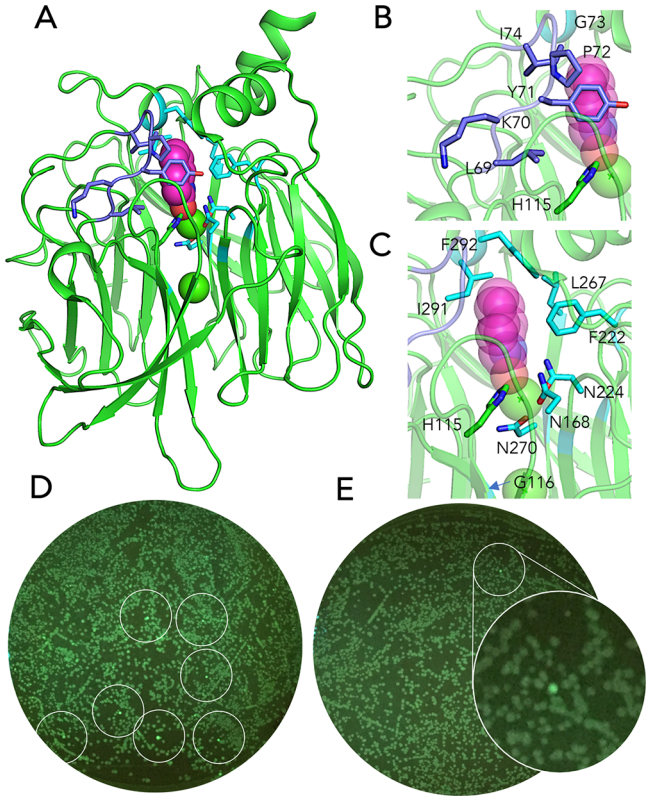

Figure 3. Structure-based PON1 library design and screening using SMC technology. (A) structure of PON1 with the bound competitive inhibitor 2HQ shown in magenta and two calcium ions shown as green spheres (PDB code 3SRG). Residue positions varied in library construction are shown in blue (Lib1) and cyan (Lib2). (B) Lib1 residue positions. (C) Lib2 residue positions. Figures were created using the PyMOL Molecular Graphics System, version 2.3.0. (D) *E. coli* DH5α cells transformed with positive-feedback plasmid expressing PON1 variants and grown on rich medium and supplemented with PXN. Several colonies (circled) show brighter fluorescence than the surrounding colonies when visualized under an illuminator (λ_{ex} = 488 nm; λ_{em} = 515 nm). (E) Lib2 colonies showing a "rare" bright colony in the whole population. The circled region is magnified in the inset for visualization of the bright colony.

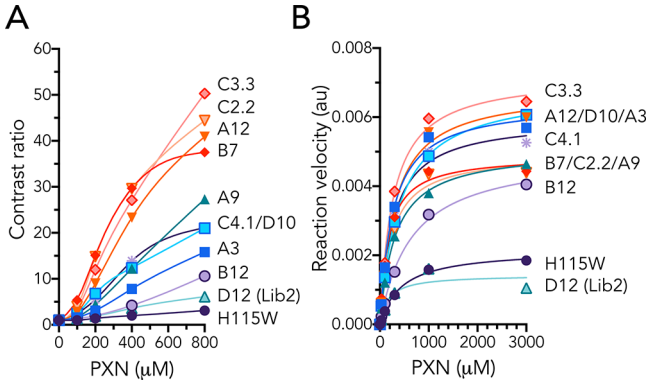

Figure 4. *In vivo* and *in vitro* activities of visually picked clones from the PON1 libraries. (A) Total activity dose−response for picked clones from the plated libraries grown in LB as a liquid culture and supplemented with PXN at various concentrations. The contrast ratio is defined as the total fluorescence of the cells in the presence of PXN over the fluorescence of the cells in the absence of PXN (background fluorescence). H115W is the scaffold on which libraries were constructed. Single PXN doses and fluorescence responses from experiments performed as biological replicates on different days are shown in Figure S2. (B) Specific activity dose−response as determined by *in vitro* spectrophotometric assay using clarified cell lysate and normalized for GFP fluorescence. A duplicate experiment performed on a different day confirmed a similar trend (Figure S4). Figures were created using GraphPad Prism, version 8.4.0.

Table 1. Observed Mutations in the Lib1 PON1 Variants and Estimated Kinetic Parameters

	amino acids at indicated positions						
variant	69	70	71	73	V_{max} (au)	K_m (μM)	fold change in k_{cat}/K_m
H115W	L	K	Y	G	0.0022	440	1
A3	V	Y	V		0.0064	263	5
A9	V	Q	I		0.0051	311	3
A12	V	L		S	0.0068	298	5
B7	V	Q	I	A	0.0049	172	6
B12	V	H	V	S	0.0050	641	2
D10	V	L			0.0068	396	3
C2.2	V	Q	V	A	0.0049	229	4
C3.3	V	Q	L	A	0.0072	268	5
C4.1	V	F	V		0.0059	268	4

Petri dish and was picked for further experimental verification (Figure 3E). The colony picking was further made more stringent by using lower PXN (100 μM) in the growth medium (data not shown).

Whole-cell catalysis and sensing using the picked clones at various concentrations of the PXN substrate showed enhanced contrast ratios (3−15-fold higher than the scaffold) for clones picked from Lib1. A single picked clone from Lib2 also showed a marginally higher contrast ratio compared with the PON1-H115W scaffold (Figures 4A and S2). The PON1 variants expressed in the clones were further tested *in vitro* by using clarified cell lysates from cultures grown in the presence of PNP inducer, which resulted in expression of the sfGFP−PON1 fusion protein. The cell lysates were normalized for sfGFP fluorescence and assayed for activity at multiple PXN concentrations. On top of the scaffold mutation (H115W), the Lib1 clones showed two to four mutations (Table 1) while Lib2-D12 also showed two mutations (F222I and F292I). Interestingly, the L69V mutation, which was present in all of the evolved Lib1 clones, has also been extensively investigated for hydrolysis of many OPs, where in the absence of H115W, a 4-fold increase in catalytic efficiency over the wild type was seen.[10] The most notable aspect of comparison between the *in vivo* activity measurements (Figure 4A) and the *in vitro* measurements (Figure 4B) is the relative ranking of the different PON1 variants. While Lib1-C3.3 did show highest V_{max} in both formats of experiment, Lib2-D12 was the lowest in both cases. Lib1-C3.3 also had the highest expression/solubility next only to the starting scaffold (showing 95% yield), Lib2-D12 showed a low 50% protein yield compared with the scaffold based on the fluorescence of the cell lysate. The solubilities of the other PON1 variants ranged between these two extreme values (Table S4 and Figure S3). The activities of the cell lysates were remeasured after storage for 3 days in a refrigerator. The results showed a very similar overall ranking of the mutants, while a consistent depletion in the activities of all the variants was also evident (Figure S4).

We further probed the contribution of the common mutation L69V in Lib1 top clones alone in the presence of the H115W

https://dx.doi.org/10.1021/acssynbio.0c00025
ACS Synth. Biol. 2020, 9, 1234−1239

mutation. Since L69 and H115 are in close proximity to each other (Cβ−Cβ distance = 5.5 Å) (Figure 3B), it was highly likely that the activity-enhancing L69V mutation (shortening of the side chain) would affect the H115W mutation (lengthening of the side chain). The whole-cell assay with the L69V mutation failed to show any significant effect on the activity (Figures S5 and S6), confirming that other discovered mutations contributed synergistically to the enhanced activity of PON1.

The SMC technology described here helps navigation through the large combinatorial space encountered during enzyme evolution. The biosensor links the total intracellular activity from the genotype to the fluorescence brightness of the cell. This enables high throughput and flexible selections, making it practical to evaluate combinatorial libraries with wide diversity and hence direct discovery of correlated mutations enhancing activity and expression. We incorporated a few key modifications from our earlier approach.[7] Here we used Petri dishes (instead of liquid culture) to minimize the cross-contamination of the formed product across cells of different genotype. We also constructed a positive-feedback circuit (instead of a dual plasmid system where the sensor and enzyme were expressed from different plasmids and enzyme expression was independent of its activity) to amplify the signal. This helped us screen a large library derived from a weak enzyme and isolate multiple mutants with improved activity. Our method was able to pull out the L69V mutation from the library and show that it was beneficial only when present with as many as one to three mutations in its vicinity. Mutations at K70 in gain-of-function strains would have been counterintuitive in structure-based design since the residue points away from the catalytic pocket (Figure 3B). With each microbial cell as a colony forming unit, the approach facilitates screening of $>10^5$ microbial colonies in a single sitting and thus can isolate the best mutations in combinatorial libraries with minimal staff, reagents, time, and instrumentation. This allowed approximately 40 000 variants of PON1 to be screened for activity in a single experiment and provided excellent reporter contrast for colony picking by eye. The SMC technology can be further adapted to a broad range of catalytic efficiencies, and various parameters like the host microbial strain (for example and not limited to *E. coli* DH5α vs JW0451), shorter incubation time, lower temperature for incubation, or lower substrate concentration can facilitate screening of enzyme libraries around high catalytic efficiency. In this study, we specifically evaluated the screening capability by building libraries with calculated diversity and demonstrated selection of "hits" from a single round of screening. Moreover, the approach and the established sensor−reporter is directly applicable to a wide range of hydrolases with available substrates that give PNP as a product.

In our current work, we observed that active mutants were indeed rare and their sequences even somewhat unexpected. While binding and stabilizing the transition state are the minimal requirements for catalysis, optimal activity comes from molecular features that are more challenging to predictively model, such as allostery, local pH, and off-target activity. Even when we know the binding mode of the enzyme, catalytic rates can be affected by second-shell or unobservable exit/entrance channel effects. These quadratically increase the number of mutable sites to consider and geometrically increase the search space for correlated mutations. We conclude that the combination of rational design for parsimonious selection of plausible mutation sites with combinatorial coverage by high-throughput experimental methods, such as the "smart" microbial cell technology described here, is a powerful yet simple approach to navigate through the sequence space efficiently.

METHODS

Paraoxon and *p*-Nitrophenol Stocks. The working stock of PXN was prepared as described previously.[7] In brief, the analytical standard paraoxon-ethyl (100 mg, Sigma-Aldrich, cat. no. 36186) was directly mixed with approximately 45 mL of water to give an 8 mM working stock. The working stock solution of PNP was made from powder (Fluka, cat. no. 1048) that was dissolved in ∼400 mM of NaOH to get a final concentration of 200 mM.

Bacterial Strains and Plasmids. The PNP sensor from the previous work, pNPmut1−1,[7] was used as the plasmid backbone for the positive-feedback plasmid (Figure S1). The genetic sequences of C-terminal His_6 tag PON1 version G3C9 (nativelike) and the H115W and V346A mutants were gifts from Prof. Dan Tawfik (Weizmann Institute of Science, Rehovot, Israel). The double-mutant genes for PON1 (H115W/V346A or H115W/L69V) were constructed using the overlap oligonucleotide assembly and extension method. The genes with terminal *Eco*RI (New England Biolabs) and AvrII (New England Biolabs) restriction endonuclease sites were double-digested with the enzymes. The *sfgfp* gene with sequence for glycine-serine linker (GGGS) and unique *Eco*RI and AvrII sites in the 3′ end replaced the original *gfp* gene in pNPmut1−1 to give a vector named sfpGLOpnpv6. The double-digested *pon1* gene insert and the vector were then ligated into circular plasmid using T4 DNA ligase (New England Biolabs). The positive-feedback plasmid with gene encoding PON1-G3C9 was dubbed sfpGlopnpv6-GGGS-pon1G3C9. The expression of sfGFP−PON1 was under the positive-feedback regulation of PON1 paraoxonase activity.

The positive-feedback plasmid sfpGlopnpv6-GGGS-pon1G3C9 and the variants with mutations in PON1 (H115W, V346A, or both) were transformed in *E. coli* cells, grown, and extracted using a commercial plasmid miniprep kit. The sequences were confirmed using Sanger sequencing (Genewiz), and the plasmids were then transformed in strain JW0451 (efflux pump component *acrB* knockout) acquired from *E. coli* Genetic Stock Center (Yale University). The chemically competent JW0451 *E. coli* cells were made following established techniques. The JW0451 strain transformed with plasmid was plated on a lysogeny broth (LB) agar plate supplemented with ampicillin (100 μg/mL) and 100−300 μM PXN or 200 μM PNP. The plates were incubated for 24−40 h at 30 °C for significant fluorescence to accumulate. The plates were illuminated using an IllumaTool lighting system (LightTools Research) equipped with an excitation wavelength of 488 nm and visualized through a 515 nm glass filter (LightTools Research). Promising colonies were grown in LB supplemented with 100 μg/mL ampicillin (LB-Amp_{100}) overnight at 30 °C, mixed with 20% glycerol, and stored at −80 °C as glycerol stocks.

Growth Medium and Whole-Cell Assay. On a regular basis, liquid cultures were grown in LB-Amp_{100}. Initial seed culture was started from a colony picked from the plate or directly from glycerol stocks and grown overnight. The seed culture was diluted 50−100-fold in fresh LB-Amp_{100} and grown for ∼3−4 h to an optical density at 600 nm (OD_{600}) of 0.4−0.6. The culture was then split in a 160 μL volume into multiple wells in a 96-deepwell plate (Nunc). The culture in each well was then induced with 40 μL of a given concentration of PNP or PXN

https://dx.doi.org/10.1021/acssynbio.0c00025
ACS Synth. Biol. 2020, 9, 1234−1239

along with $CaCl_2$ at a final concentration of 1 mM and then grown overnight at 25 °C under vigorous shaking using a deepwell maximizer shaker (Taitec Bioshaker MBR-022UP). The next day, cells were diluted 50−100-fold in 1× PBS and then analyzed using a flow cytometer (LSR II or Accuri C6, BD Biosciences) with standard settings for GFP measurement (excitation at 488 nm, emission at 525/50 nm for LSRII or excitation at 488 nm and emission at 533/30 nm for Accuri C6). The mean fluorescence value of 100 000 cells was used for comparison.

Library Synthesis and Screening. The PON1 gene libraries Lib1 and Lib2 were synthesized using oligonucleotides with appropriate wobbles in codons (Tables S2 and S3). The gene sequence for PON1-H115W was used as the template. Fragments of gene with specific diversification were first created using PCR and then assembled using the overlap oligonucleotide assembly and extension method. The diversified genetic libraries were then double-digested using restriction endonuclease enzymes *Eco*RI and AvrII and then ligated into the vector sfpGLOpnpv6 plasmid double-digested with same restriction endonucleases. The plasmid libraries were transformed in commercially available high-efficiency ElectroMax DH5α-E electrocompetent cells (Thermo Scientific), plated on LB agar−Amp_{100} plates, and incubated at 37 °C overnight. The colonies were scraped and mixed with glycerol (20% v/v) and stored in −80 °C as glycerol stocks.

The scraped colonies were also diluted appropriately in LB and plated on LB agar−Amp_{100} plates supplemented with 330 μM PXN and 1 mM $CaCl_2$. The plates were incubated at 30 °C for 40 h, and colonies were visualized using the IllumaTool lighting system for GFP fluorescence as described earlier.

The colonies with high fluorescence were picked for further analysis. To avoid any cross-contamination from neighboring colonies, each picked colony was streaked on an LB agar−Amp_{100} plate and incubated at 30 °C for 16−24 h, and then four to six well-separated colonies were picked and tested in liquid culture as described earlier.

Cell Lysis and *In Vitro* Paraoxonase Assay. The DH5α clones expressing the promising PON1 variants were grown in 5 mL of LB-Amp_{100} liquid cultures. At an OD_{600} of ∼0.6, the cells were induced with 200 μM PNP, since the sfGFP−PON1 fusion was more uniformly expressed from the P_{pob} promoter when induced by PNP. After overnight induction at 20 °C and shaking at 225 rpm, the cells were spun down. The pellets were stored in −80 °C until needed for next step. In order to lyse the cells, each frozen cell pellet was thawed, treated with approximately 200 μL of Bugbuster cell lysis solution (Sigma) and Benzonase (250 units; Sigma), and incubated under gentle shaking for 30 min at room temperature. The cell lysate was clarified by centrifugation at >16000*g* and 4 °C. The supernatants were immediately transferred to another set of Eppendorf tubes for storage at 4 °C and experimental use.

PON1 enzyme was estimated by measuring GFP fluorescence in each cell lysate using a Synergy H4 microplate reader (BioTek). Cell lysates were diluted 10-fold using the dilution buffer (25 mM Tris-HCl, pH 8.0, 100 mM NaCl). Next, 12.5 μL aliquots of the diluted cell lysates were used in 100 μL reactions in a 96-well plate (Nunc). The final reaction buffer composition was maintained at 25 mM Tris-HCl, pH 8.0, 100 mM NaCl, 1 mM $CaCl_2$, and 1 mM TCEP reducing agent. Various final concentrations of PXN (30−3000 μM) were used for each cell lysate. Reaction rates were measured as the increase in absorbance at 405 nm (quantifying PNP formation) per unit time using the Synergy H4 microplate reader. The reaction rates were then normalized to the PON1 concentration using the GFP fluorescence value for each cell lysate. The linear reaction rate at each PXN concentration was plotted against the starting PXN concentration to obtain a Michaelis−Menten plot.

■ ASSOCIATED CONTENT

Supporting Information

The Supporting Information is available free of charge at https://pubs.acs.org/doi/10.1021/acssynbio.0c00025.

Raw fluorescence data and library details (Tables S1−S4); plasmid map, supporting experiments, and dose−response plots (Figures S1−S6) (PDF)

■ AUTHOR INFORMATION

Corresponding Authors

Ramesh K. Jha − *Bioscience Division, Los Alamos National Laboratory, Los Alamos, New Mexico 87545, United States;* orcid.org/0000-0001-5904-3441; Email: rjha@lanl.gov

Charlie E. M. Strauss − *Bioscience Division, Los Alamos National Laboratory, Los Alamos, New Mexico 87545, United States;* Email: cems@lanl.gov

Complete contact information is available at: https://pubs.acs.org/10.1021/acssynbio.0c00025

Funding

Financial support was provided by the Defense Threat Reduction Agency (CBCALL12-LS6-1-0622).

Notes

The authors declare the following competing financial interest(s): Modified biosensors and biocatalysts and methods of use are subjects of patent applications by Los Alamos National Laboratory.

■ ACKNOWLEDGMENTS

The authors thank Prof. Dan Tawfik (Weizmann Institute of Science) for the kind gift of *pon1* genes (G3C9 and the H115W and V346A mutants).

■ ABBREVIATIONS

sfGFP, superfolder green fluorescent protein; PNP, *p*-nitrophenol; PXN, paraoxon; SMC, smart microbial cell; OP, organophosphate.

■ REFERENCES

(1) Sio, C. F., and Quax, W. J. (2004) Improved β-Lactam Acylases and Their Use as Industrial Biocatalysts. *Curr. Opin. Biotechnol. 15* (4), 349−355.

(2) André, I., Potocki-Véronèse, G., Barbe, S., Moulis, C., and Remaud-Siméon, M. (2014) CAZyme Discovery and Design for Sweet Dreams. *Curr. Opin. Chem. Biol. 19*, 17−24.

(3) Jaeger, K.-E., and Reetz, M. T. (1998) Microbial Lipases Form Versatile Tools for Biotechnology. *Trends Biotechnol. 16* (9), 396−403.

(4) Ghanem, E., and Raushel, F. M. (2005) Detoxification of Organophosphate Nerve Agents by Bacterial Phosphotriesterase. *Toxicol. Appl. Pharmacol. 207* (2, Suppl.), 459−470.

(5) Bunzel, H. A., Garrabou, X., Pott, M., and Hilvert, D. (2018) Speeding up Enzyme Discovery and Engineering with Ultrahigh-Throughput Methods. *Curr. Opin. Struct. Biol. 48*, 149−156.

(6) Goddard, J.-P., and Reymond, J.-L. (2004) Recent Advances in Enzyme Assays. *Trends Biotechnol. 22* (7), 363−370.

(7) Jha, R. K., Kern, T. L., Kim, Y., Tesar, C., Jedrzejczak, R., Joachimiak, A., and Strauss, C. E. M. (2016) A Microbial Sensor for

Organophosphate Hydrolysis Exploiting an Engineered Specificity Switch in a Transcription Factor. *Nucleic Acids Res. 44* (17), 8490−8500.
(8) Harel, M., Aharoni, A., Gaidukov, L., Brumshtein, B., Khersonsky, O., Meged, R., Dvir, H., Ravelli, R. B. G., McCarthy, A., Toker, L., Silman, I., Sussman, J. L., and Tawfik, D. S. (2004) Structure and Evolution of the Serum Paraoxonase Family of Detoxifying and Anti-Atherosclerotic Enzymes. *Nat. Struct. Mol. Biol. 11* (5), 412−419.
(9) Aharoni, A., Gaidukov, L., Yagur, S., Toker, L., Silman, I., and Tawfik, D. S. (2004) Directed Evolution of Mammalian Paraoxonases PON1 and PON3 for Bacterial Expression and Catalytic Specialization. *Proc. Natl. Acad. Sci. U. S. A. 101* (2), 482−487.
(10) Amitai, G., Gaidukov, L., Adani, R., Yishay, S., Yacov, G., Kushnir, M., Teitlboim, S., Lindenbaum, M., Bel, P., Khersonsky, O., Tawfik, D. S., and Meshulam, H. (2006) Enhanced Stereoselective Hydrolysis of Toxic Organophosphates by Directly Evolved Variants of Mammalian Serum Paraoxonase: Enhanced Stereoselective OP Hydrolysis by PON1. *FEBS J. 273* (9), 1906−1919.
(11) Gupta, R. D., Goldsmith, M., Ashani, Y., Simo, Y., Mullokandov, G., Bar, H., Ben-David, M., Leader, H., Margalit, R., Silman, I., Sussman, J. L., and Tawfik, D. S. (2011) Directed Evolution of Hydrolases for Prevention of G-Type Nerve Agent Intoxication. *Nat. Chem. Biol. 7* (2), 120−125.
(12) Gupta, R. D., and Tawfik, D. S. (2008) Directed Enzyme Evolution via Small and Effective Neutral Drift Libraries. *Nat. Methods 5* (11), 939−942.
(13) Cherny, I., Greisen, P., Ashani, Y., Khare, S. D., Oberdorfer, G., Leader, H., Baker, D., and Tawfik, D. S. (2013) Engineering V-Type Nerve Agents Detoxifying Enzymes Using Computationally Focused Libraries. *ACS Chem. Biol. 8* (11), 2394−2403.
(14) Jha, R. K., Narayanan, N., Pandey, N., Bingen, J. M., Kern, T. L., Johnson, C. W., Strauss, C. E. M., Beckham, G. T., Hennelly, S. P., and Dale, T. (2019) Sensor-Enabled Alleviation of Product Inhibition in Chorismate Pyruvate-Lyase. *ACS Synth. Biol. 8* (4), 775−786.
(15) Williams, T. C., Xu, X., Ostrowski, M., Pretorius, I. S., and Paulsen, I. T. (2017) Positive-Feedback, Ratiometric Biosensor Expression Improves High-Throughput Metabolite-Producer Screening Efficiency in Yeast. *Synth. Biol. 2* (1), ysw002.
(16) Waldo, G. S., Standish, B. M., Berendzen, J., and Terwilliger, T. C. (1999) Rapid Protein-Folding Assay Using Green Fluorescent Protein. *Nat. Biotechnol. 17* (7), 691−695.
(17) Pédelacq, J.-D., Cabantous, S., Tran, T., Terwilliger, T. C., and Waldo, G. S. (2006) Engineering and Characterization of a Superfolder Green Fluorescent Protein. *Nat. Biotechnol. 24* (1), 79−88.
(18) Baba, T., Ara, T., Hasegawa, M., Takai, Y., Okumura, Y., Baba, M., Datsenko, K. A., Tomita, M., Wanner, B. L., and Mori, H. (2006) Construction of *Escherichia Coli* K-12 in-Frame, Single-Gene Knockout Mutants: The Keio Collection. *Mol. Syst. Biol. 2*, 2006.0008.
(19) Ben-David, M., Elias, M., Filippi, J.-J., Duñach, E., Silman, I., Sussman, J. L., and Tawfik, D. S. (2012) Catalytic Versatility and Backups in Enzyme Active Sites: The Case of Serum Paraoxonase 1. *J. Mol. Biol. 418* (3−4), 181−196.

https://dx.doi.org/10.1021/acssynbio.0c00025
ACS Synth. Biol. 2020, 9, 1234−1239